24th COBEM - 2017

24th ABCM International Congress of Mechanical Engineering
December 3-8, 2017, Curitiba, PR, Brazil

COBEM-2017-0982
EXPERIMENTAL IMAGE ANALYSIS OF GAS BUBBLES PATH LINE IN CENTRIFUGAL PUMP IMPELLER

Rodolfo Marcilli Perissinotto
Jonathan Saturnino
William Monte Verde
Jorge Luiz Biazussi
Marcelo Souza de Castro
Antonio Carlos Bannwart
School of Mechanical Engineering, University of Campinas - UNICAMP
Rua Mendeleyev, 200 - Cidade Universitária, Campinas-SP, Brasil, CEP 13083-860
rodolfoperissinotto@gmail.com
jonathanadley@hotmail.com
williammonteverde@gmail.com
jorge.biazussi@gmail.com
mcastro@fem.unicamp.br
bannwart@fem.unicamp.br

Abstract. *The main objective of this research is to analyze the path line and the velocity of air bubbles flowing within an Electrical Submersible Pump (ESP) impeller operating with a two-phase gas-liquid flow, under various conditions. In this paper, a digital image processing was performed, based on the experimental study of Monte Verde et al. (2017). Results for a population of air bubbles reveal that they present random trajectories, with a chaotic behavior. Comparison between air bubbles on the suction blade and on the pressure blade suggests that the velocity of air bubbles is dependent on their position within the channel and also on the water flow rate associated with diverse flow patterns. The air bubbles take milliseconds to traverse the channels, at velocities in the order of units of meters per second. The water flow carries the air bubbles from the channel inlet to the outlet. Fluid-particle interactions are relevant to the air bubble behavior.*

Keywords: *Electrical Submersible Pump, Two-Phase Gas-Liquid Flow, Flow Visualization, Gas Bubbles.*

1. INTRODUCTION

The Electrical Submersible Pump (ESP) is a multiple stage centrifugal pump used as an artificial lift method to increase the oil production by adding pressure energy to the fluid. Each stage has an impeller and a diffuser. According to Andriolli (2016), the ESP is widely used in wells with low and high liquid flow rates, from 50 m³/d to over 5000 m³/d, onshore and offshore. It is estimated between 150,000 and 200,000 wells in operation with ESPs all around the world, as reported by Flatern (2015). The ESP is frequently used for viscous oil due to the low efficiency of the gas lift methods.

When the pressure inside the well is less than the oil saturation pressure, the produced fluid becomes a two-phase gas-liquid mixture, composed of gas bubbles in a carrier liquid. The presence of a compressible phase affects the centrifugal pump performance and causes operational instabilities which can lead to the reduction of the ESP life time. The physical understanding of the flow within ESPs is fundamental to improve the available technology and develop efficient pumps.

In this work, an experimental image analysis is conducted in order to investigate the motion of gas bubbles within an ESP impeller under different operating conditions. Photographs acquired by Monte Verde *et al.* (2017) were used in this paper. The main objective is to observe the trajectories of gas bubbles and evaluate their velocities. The determination of velocities is the first step to estimate the drift between phases and the drag force that carries the gas bubbles out of the impeller channels.

This paper is organized into some sections: this introduction, a short literature review, a description of the procedure adopted to process the images, a discussion about the main results and the most important conclusions.

2. LITERATURE REVIEW

In the last decades, many researchers dedicated themselves to the study of centrifugal pumps working with two-phase gas-liquid flows. Most authors investigated the performance of centrifugal pumps and the instabilities observed when the device is working with presence of gas. Other authors analyzed the flow patterns that occur within the pumps, using flow visualization techniques, especially high-speed cameras. Some researchers also studied the behavior of gas bubbles in the impeller of centrifugal pumps and the forces that govern their movement.

Murakami and Minemura (1977) explored the trajectories of isolated air bubbles in a rotating impeller and their effect on the pump performance. The researchers noticed that the air bubbles follow substantially the same path as water. In addition, the authors observed that the pump performance is reduced when the quantity of air is increased, leading to discontinuities in the pressure curves. Years later, the discontinuities would be called surging and gas locking.

Estevam (2002) developed the first visualization prototype for the petroleum industry, with an impeller made with a transparent material. The researcher observed the formation of stationary bubbles within the impeller channels. The author also noticed a dependence between the air bubble diameter and the pump pressure generation. Estevam (2002) proposed a phenomenological model and obtained dimensionless numbers that indicate which type of flow occurs in the impeller.

Biazussi (2014) performed tests in three ESPs operating with air-water mixtures, in order to understand the physical phenomena involved in flows with presence of gas. The author proposed single-phase and two-phase drift models for the performance curves and found satisfactory results with deviations lower than 10%.

Sabino (2015) visualized the movement of individual air bubbles in a water flow within a rotating impeller. The author identified the typical trajectories of some bubbles. In general, their movement is parallel and close to the suction blade. However, some bubbles deviate to the channel center or to the pressure blade. Sabino (2015) also calculated the velocity of some bubbles as a function of their position inside the channels. The velocity of the bubbles presents a chaotic behavior. The air velocity is similar to water velocity, but the bubbles near the suction blade have higher velocities than the bubbles distant from the same blade.

Monte Verde (2016) worked on two experimental facilities. The author investigated the influence of elements such as viscosity, surface tension, rotation speed, intake pressure, liquid flow rate and pump inclination on the ESP performance operating with two-phase gas-liquid flows. The researcher also proposed a model based on Gülich (2008), extended for viscous fluids. Regarding flow visualization, the researcher identified four flow patterns and observed phenomena such as accumulation, agglomeration and coalescence of gas bubbles.

One year later, Cubas Cubas (2017) also evaluated the performance of a centrifugal pump operating with a two-phase air-water flow. The researcher obtained high-speed images using a prototype with transparent impeller and diffuser. The author associated the photographs to the instabilities observed in the performance curves.

As discussed, many authors studied centrifugal pumps working with two-phase gas-liquid flows. The behavior of gas bubbles seems to define the flow pattern and the pump performance. This paper extends the phenomenological analysis of gas bubbles motion inside the channels of an ESP. The intention is to go a little deeper in the understanding of what really happens to the bubbles in a centrifugal pump operating in presence of gas.

3. EXPERIMENTAL PROCEDURE

Experiments were performed at University of Campinas, in Brazil, by Monte Verde *et al.* (2017) and their results were used in this paper. Air and water were chosen to compose the gas-liquid flow. A high-speed camera *Olympus I-SPEED 3* was selected as the flow visualization technique. It has a maximum resolution of 1280 x 1024 pixels at 2000 fps acquisition rate. The tests were carried out at different rotational speeds, water flow rates and gas fractions, but this study focuses on a single experiment with the following characteristics: ESP rotation speed of 900 rpm, air flow rate of 0.050 kg/h and water flow rates varying from 1.2 to 5.2 approximately.

The researchers designed and built an ESP prototype which allows the flow visualization through a transparent shell made with organic glass. The prototype was based on the *Baker-Hughes P23* electrical submersible pump. In addition to the ESP prototype, the complete experimental facility is composed of water and air flow lines. The Fig. 1 shows a photo of the experimental assembly and the Fig. 2 presents a schematic layout.

A booster pump takes the water out of the tank. The water passes through a heat exchanger and a Coriolis flow meter. Then, the water reaches the prototype intake. Meanwhile, the air is compressed by a compressor and stored in a vessel. The compressed air flows through a laminar flow meter and is finally injected in the prototype intake, through an injector. The mixture occurs next to the pump suction, in order to avoid segregation between gas and liquid. The mixture passes through the ESP impeller and then is pumped back to the tank, where the fluids are gravitationally separated.

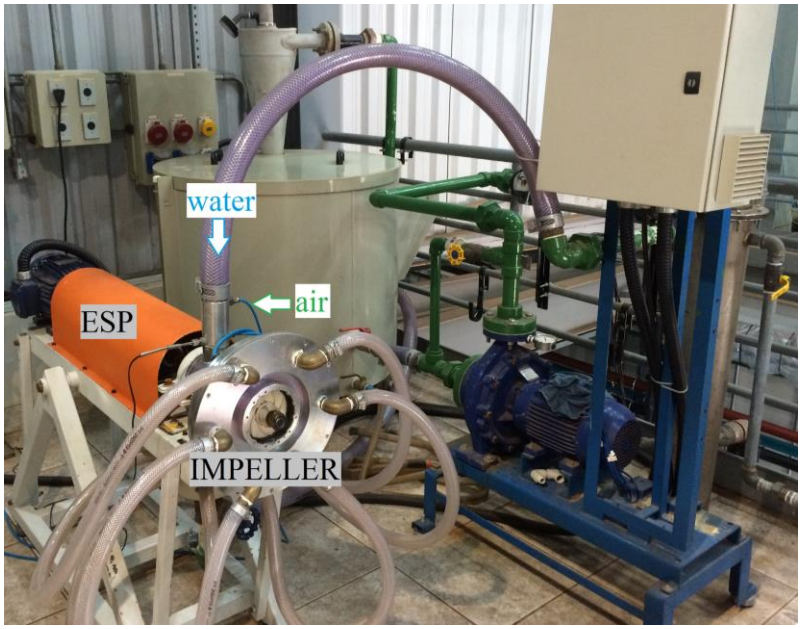

Figure 1. Photo of the experimental loop

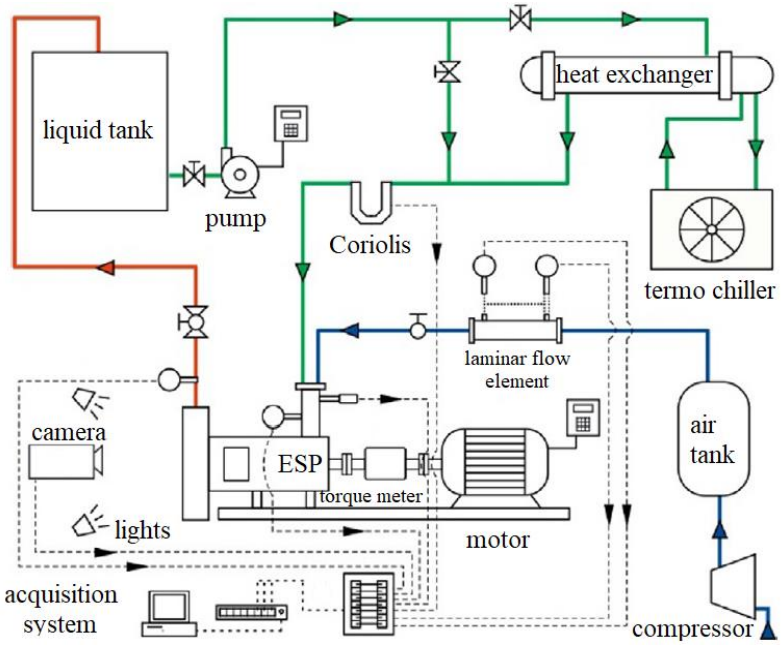

Figure 2. Schematic diagram of the test bench

4. RESULTS AND DISCUSSION

This study aims to analyze the behavior of air bubbles within the impeller channels at some operational points of the ESP prototype operating with a two-phase air-water mixture. As mentioned before, the images were collected by Monte Verde *et al.* (2017) and each photograph set refers to a distinct operational point, as Fig. 3 shows. The conditions IM1 to IM11 are associated to different flow patterns. As the liquid flow rate decreases, the air bubbles become larger and affect the pump performance. Instabilities occur at IM7, which defines the surging point. The gas locking occurs at IM11.

The images were processed to enable the investigation of the trajectories and velocities. The impeller rotation was removed and the air bubbles were tracked using the software *IDT Motion Studio*, which determines the particle position R and θ in a polar non-inertial coordinate system, by identifying differences between consecutive images. Then, the position is numerically differentiated and velocity V is obtained, as described by Eq. (1).

$$\mathrm{V} = V_R\,\hat{\imath}_\mathrm{R} + V_\theta\,\hat{\imath}_\theta = \dot{R}\,\hat{\imath}_\mathrm{R} + R\dot{\theta}\,\hat{\imath}_\theta \tag{1}$$

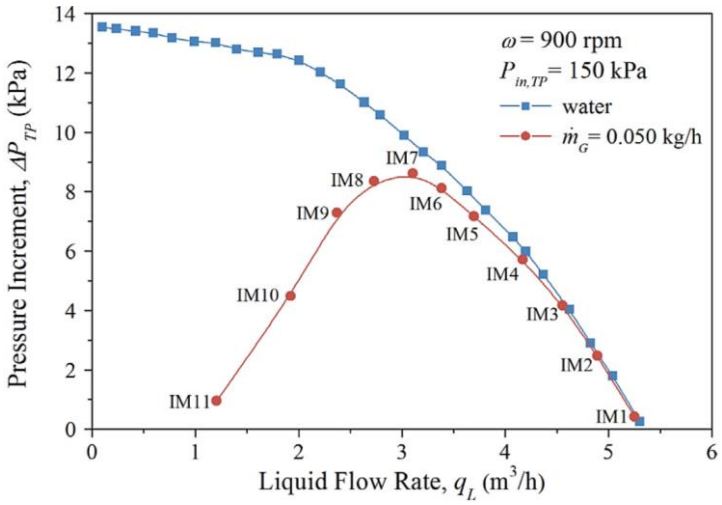

Figure 3. Performance of the centrifugal pump operating with a two-phase air-water flow at constant rotation speed, gas flow rate and intake pressure (Monte Verde *et al.*, 2017)

As already mentioned, the conditions shown in Fig. 3 are associated to flow patterns visualized and classified by Monte Verde *et al.* (2017): bubble flow (IM1, IM2, IM3), agglomerated bubble flow (IM4, IM5), gas pocket flow (IM6, IM7, IM8) and segregated flow (IM9, IM10, IM11). As the liquid flow rate decreases, the amount of bubbles inside the impeller becomes greater, the interaction among them increases, the gas accumulation gets intensified and, therefore, the bubble tracking becomes more difficult. The air bubbles were tracked at the conditions IM1 to IM8. The conditions IM9, IM10 and IM11 could not be investigated because the segregated flow pattern is characterized by elongated air bubbles that remain stationary and occupy most of the channel transversal section, making the tracking impossible.

4.1 Path Line

The air bubbles exhibit random trajectories, with a chaotic behavior. However, a pattern is observed in all the operating conditions. Many air bubbles perform the path presented in Fig. 4. The air bubbles enter the channel and stay close to the suction blade, but suffer a deviation next to the outlet, to the pressure blade direction, passing through the channel center. It suggests the existence of phenomena associated to the turbulent flow, as recirculation, on the tip of the suction blade. Some air bubbles move close to the suction blade and leave the channel without undergoing deviations. Similarly, a few bubbles move near the pressure blade. Lateral deviations are observed in all directions.

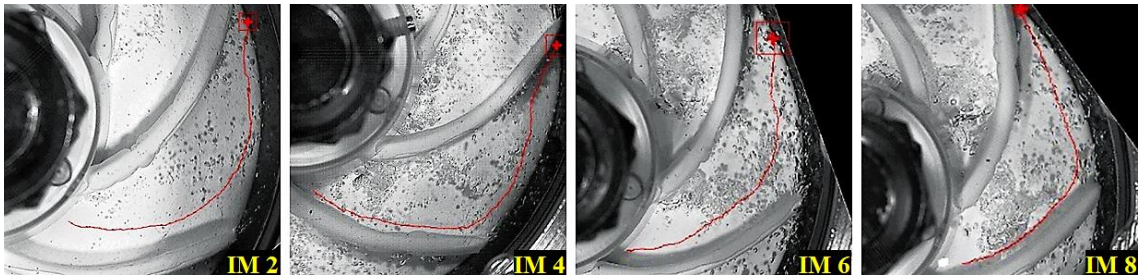

Figure 4. Usual path of air bubbles: deviation from the suction to the pressure blade

Coalescence is observed at the conditions IM6, IM7 and IM8, related to the gas pocket flow pattern. In general, small fast bubbles collide with large slow bubbles and they become a new air bubble. In this case, the bubble cannot be tracked from the channel inlet to the outlet, but only until the coalescence occurs. Some examples can be seen in Fig. 5.

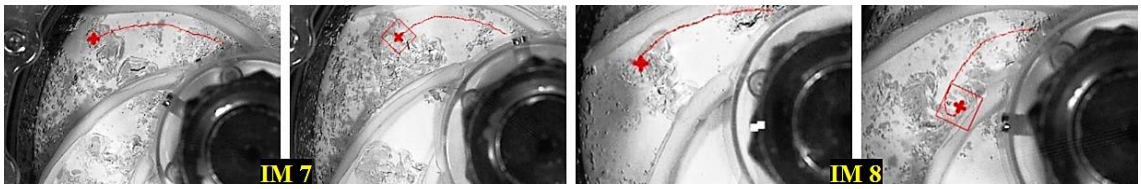

Figure 5. Incomplete path of air bubbles: collision and coalescence within the channel

4.2 Velocity

Air bubbles that move close to the blades are further analyzed in the next paragraphs, which discuss the velocities for samples of 13 bubbles at IM2, IM5 and IM8.

4.2.1 Same condition, different trajectory

Four bubbles were tracked at IM2, the bubble flow pattern. Their trajectories have a length of 0.046 meter on average and their position within the channels are presented in Fig. 6. It is observed that two bubbles move near the suction blade and the other two bubbles move next to the pressure blade. The impeller rotates clockwise.

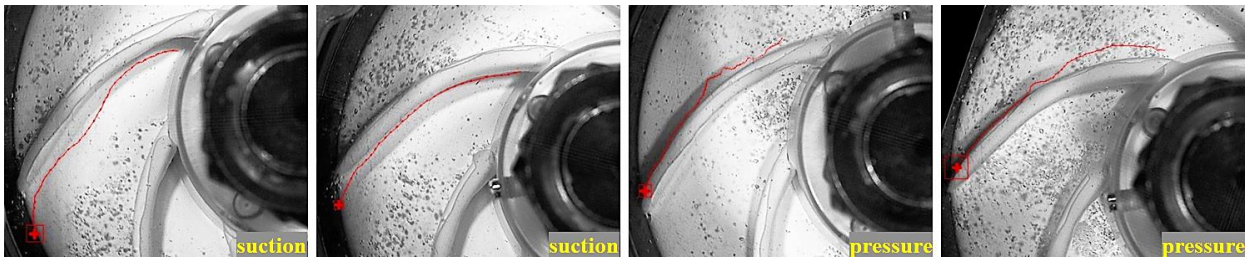

Figure 6. Air bubbles at IM2 with trajectories close to the suction and pressure blades

The air bubbles on the suction blade take 0.016 second to traverse the channel, while the air bubbles on the pressure blade take 0.039 second on average. Thus, the suction-bubbles move faster than the pressure-bubbles, as Fig. 7 displays.

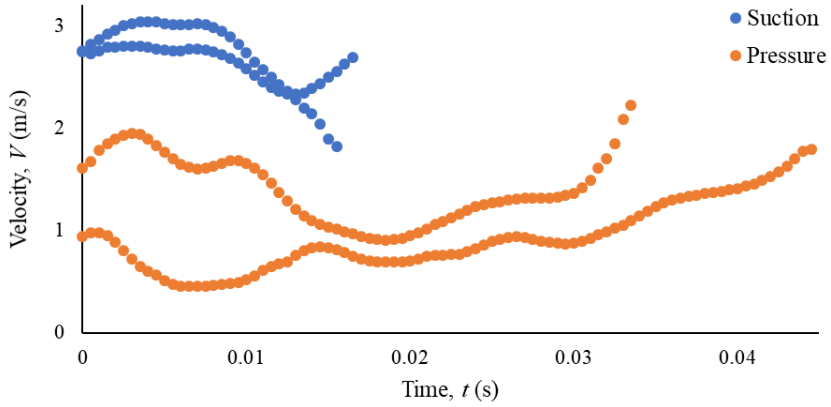

Figure 7. Resultant velocities of air bubbles at IM2 with trajectories on suction and pressure blades

The velocity of bubbles on the suction blade have a magnitude of 2.60 m/s on average. On the other hand, the bubbles on the pressure blade present an average velocity of 1.12 m/s. The magnitude of the velocity vector is exhibited in Fig. 8, with polynomial fits. The dimensionless radius R^* varies from 0 (channel inlet) to 1 (channel outlet).

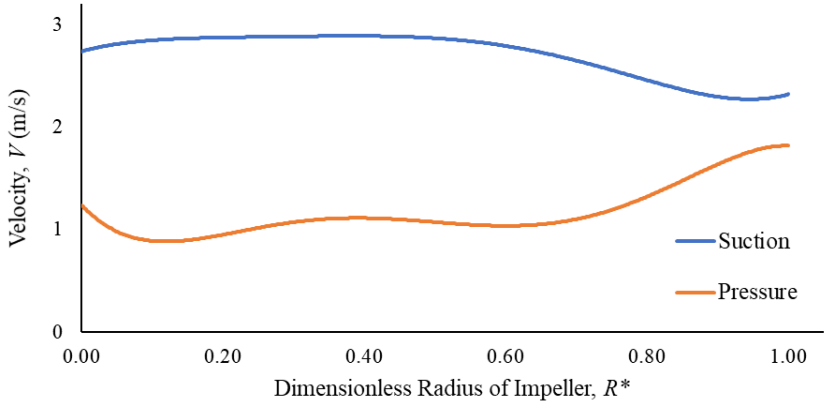

Figure 8. Average velocities of air bubbles at IM2 with trajectories on suction and pressure blades

The results suggest the existence of a velocity profile for water, acting on the transversal section of the channels. The water flows faster in the suction region, so the air bubbles also go fast, since they are carried by water. The continuous liquid is responsible for the movement of the disperse gas. The fluid-particle interaction is described with forces such as the drag force. Table 1 resumes the results.

Table 1. Results for air bubbles at IM2 with trajectories on suction and pressure blades

Air bubble	Position within the channel	Length of trajectory (m)	Time to move through the channel (s)	Average velocity (m/s)
Bubble 1	Suction blade	0.043	0.017	2.55
Bubble 2		0.042	0.016	2.64
Bubble 3	Pressure blade	0.041	0.045	0.88
Bubble 4		0.047	0.034	1.38

4.2.2 Same trajectory, different condition

Nine bubbles were tracked at IM2, IM5 and IM8, three different patterns. Their trajectories are near the suction blade with an average length of 0.044 meter. The air bubbles at IM2 take 0.016 second to traverse the channel, while the air bubbles at IM8 take 0.024 second on average to pass through the impeller. Bubbles at IM2 move faster than bubbles at IM5, which move faster than bubbles at IM8, as Fig. 9 illustrates.

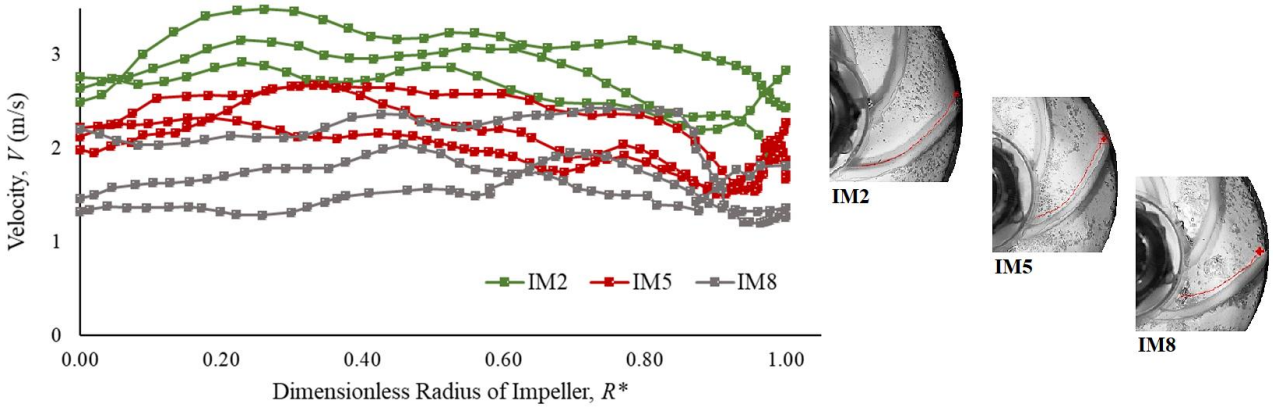

Figure 9. Resultant velocities of air bubbles at IM2, IM5 and IM8 with trajectories on suction blades

The velocity of bubbles at IM2 present a magnitude of 2.80 m/s on average. On the other hand, the bubbles at IM8 have an average velocity of 1.72 m/s. The magnitude of the velocity vector is shown in Fig. 10, with polynomial fits. The dimensionless radius R^* varies from 0 to 1, the channel inlet and outlet.

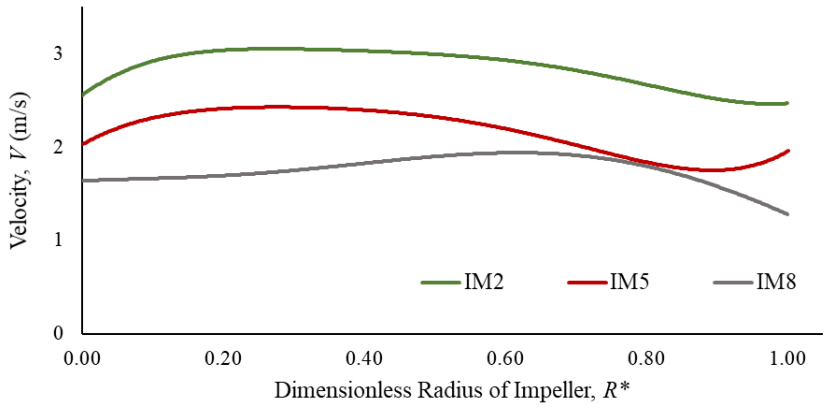

Figure 10. Average velocities of air bubbles at IM2, IM5 and IM8 with trajectories on suction blades

The results reveal a dependence between the air bubble velocity and the water flow rate. As the liquid flow increases, the fluid flows faster and pushes the air bubbles with higher speed. The carrier liquid governs the movement of the disperse gas, through fluid-particle interactions as the drag force, mentioned before. The forces that govern the bubble motion are further analyzed by Minemura and Murakami (1980).

When the velocity of water is known, the slip between phases can be calculated and the drift model can be used to describe the flow. Besides the fluid-particle interactions, there are also particle-wall and particle-particle interactions, as explained by Crowe *et al*. (1998). Essentially, the air bubbles collide with other bubbles and with the blades, leading to changes in their velocities.

5. CONCLUSIONS

The image analysis reveals that most air bubbles perform random trajectories. Many bubbles enter the channel near the suction blade, but suffer a deviation to the pressure blade direction. Some bubbles stay close to the suction blade and do not undergo deviations. A few bubbles move near the pressure blade as well.

The image processing also exposes quantitative results. The velocity of air bubbles seems dependent on their position within the channel and also on the water flow rate related to the flow patterns and the operating conditions. The bubbles take around 20 or 30 milliseconds to move from the channel inlet to the outlet, performing paths with 40 millimeters approximately, at average velocities in the order of 1.0 to 3.0 meters per second. The water flow carries the air bubbles. Fluid-particle interactions exist in all conditions, in the whole impeller. The bubble motion is governed by water velocity profile, drag force and phenomena associated to the turbulence.

Particle-particle interactions also occur, especially when the water flow rate decreases. In this case, the quantity of bubbles increases and the gas accumulation becomes more intense. Coalescence is observed. Small fast bubbles collide with large slow bubbles and they become new air bubbles.

6. ACKNOWLEDGEMENTS

The authors thank Statoil Brazil, ANP ("Compromisso de Investimentos com Pesquisa e Desenvolvimento") and PRH/ANP for providing financial support for this work. Acknowledgments are also extended to CEPETRO/UNICAMP and ALFA - Artificial Lift & Flow Assurance Research Group.

7. REFERENCES

Andriolli, I. “Introdução à Elevação e Escoamento Monofásico e Multifásico de Petróleo”. Interciência, 2016.

Biazussi, J. “Modelo de deslizamento para escoamento gás-líquido em bombas centrífugas submersas operando com fluido de baixa viscosidade”. PhD thesis. School of Mechanical Engineering, University of Campinas, Brazil, 2014.

Crowe, C., Sommerfeld, M., Tsuji, Y. “Multiphase Flows with Droplets and Particles”. Boca Raton: CRC Press, 1998.

Cubas Cubas, J. “Estudo experimental do escoamento bifásico ar-água em uma bomba centrífuga radial”. Master’s thesis. Federal University of Technology - Paraná, Brazil, 2017.

Estevam, V. “Uma análise fenomenológica da operação de bomba centrifuga com escoamento bifásico”. PhD thesis. School of Mechanical Engineering, University of Campinas, Brazil, 2002.

Flatern, R. “The Defining Series - Electrical Submersible Pumps”, Oilfield Review, 2015.

Gülich, J. “Centrifugal Pumps”. Berlin: Springer, 2008.

Minemura, K., Murakami, M. “A theoretical study on air bubble motion in a centrifugal pump impeller”, Journal of Fluids Engineering, Vol. 102, p. 446-455, 1980.

Monte Verde, W. “Bombas centrífugas submersas: visualização do escoamento bifásico gás-líquido, operação com fluido viscoso e modelagem de desempenho”. PhD thesis. School of Mechanical Engineering, University of Campinas, Brazil, 2016.

Monte Verde, W., Biazussi, J., Sassim, N., Bannwart, A. “Experimental study of gas-liquid two-phase flow patterns within centrifugal pumps impellers”. Experimental Thermal and Fluid Science, Vol. 85, pp. 37-51, 2017.

Murakami, M., Minemura, K. “Flow of air bubbles in centrifugal impellers and its effect on the pump performance”. 6th Australasian Hydraulics and Fluid Mechanics Conference, Adelaide, Australia, 1977.

Sabino, R. “Análise da dinâmica de uma bolha de gás em uma bomba centrífuga”. Master’s thesis. Federal University of Technology - Paraná, Brazil, 2015.

8. RESPONSIBILITY NOTICE

The authors are the only responsible for the printed material included in this paper.